TOXICOLOGICAL SCIENCES **118(2)**, 704–715 (2010)
doi:10.1093/toxsci/kfq262
Advance Access publication September 6, 2010

Analysis of the CYP1A1 mRNA Dose-Response in Human Keratinocytes Indicates that Relative Potencies of Dioxins, Furans, and PCBs Are Species and Congener Specific

Carrie H. Sutter,*[,1] Sridevi Bodreddigari,* Thomas R. Sutter,* Erik A. Carlson,† and Jay B. Silkworth†

*Department of Biological Sciences and W. Harry Feinstone Center for Genomic Research, University of Memphis, Memphis, Tennessee 38152-3560; and †General Electric Company, Global Research Center, Environmental Technology Laboratory, One Research Circle, Niskayuna, New York 12309

[1]To whom correspondence should be addressed at Department of Biological Sciences and W. Harry Feinstone Center for Genomic Research, University of Memphis, 201 Life Sciences Building, Memphis, TN 38152-3560. Fax: (901) 678-2458. E-mail: csutter@memphis.edu.

Received June 15, 2010; accepted August 18, 2010

Reports indicate that toxic equivalency factors (TEFs) based primarily on rodent data do not accurately predict *in vitro* human responsiveness to certain dioxin-like chemicals (DLCs). To investigate this in cells responsive to dioxins and relevant to chloracne, normal human epidermal keratinocytes were treated with 2,3,7,8-tetrachlorodibenzo-*p*-dioxin (TCDD) and several DLCs, each with a TEF value of 0.1, representing three classes of congeners. We estimated half maximal effective concentration (EC50)–based donor-specific relative potency (REP) values for cytochrome P450 1A1 (*CYP1A1*) messenger RNA (mRNA) induction for TCDD, 1,2,3,6,7,8-hexachlorodibenzo-*p*-dioxin (HxCDD), 2,3,7,8-tetrachlorodibenzofuran (TCDF), 1,2,3,6,7,8-hexachlorodibenzofuran (HxCDF), and 3,3′,4,4′,5-pentachlorobiphenyl (PCB 126). We also determined EC50-based population-level REP values ($n = 4$) for *CYP1A1* mRNA induction for TCDD, HxCDF, and PCB 126. Furthermore, an alternative factor, the relative threshold factor (RTF) based on the low end (threshold) of the dose-response curve, was calculated. Our results demonstrated that HxCDF had a population-based REP value of 0.98, 9.8-fold higher than its assigned TEF value of 0.1. Conversely, PCB 126 had an REP value of 0.0027 and an RTF of 0.0022, 37-fold and 45-fold less than its assigned TEF of 0.1, respectively. The REP values for HxCDD and TCDF were 0.24 and 0.10, respectively, similar to their assigned value of 0.1. Therefore, although the DLCs tested in the current study all possessed the same assigned TEF value of 0.1, congener-specific differences in REPs and RTFs were observed for human keratinocytes. These congener-specific discrepancies are likely because of differences in interspecies factors that have yet to be defined.

Key Words: **TCDD; PCB; toxic equivalency factor; human; keratinocyte; chloracne; threshold; human health risk assessment.**

The estimation of risk to human health from exposure to environmental contaminants such as polychlorinated dibenzo-*p*-dioxins, polychlorinated dibenzofurans (PCDFs), and polychlorinated biphenyls (PCBs) is currently based on the potency of these chemicals in nonhuman animal models of toxicity. For risk assessment purposes, these dioxin-like chemicals (DLCs) are assigned toxic equivalency factor (TEF) values relative to 2,3,7,8-tetrachlorodibenzo-*p*-dioxin (TCDD) by the World Health Organization (WHO) (Van den Berg *et al.*, 2006). These values have been generated predominantly from results of *in vitro* and *in vivo* rodent experiments measuring events downstream of activation of the aryl hydrocarbon receptor (AHR) (Haws *et al.*, 2006). However, a number of studies indicate that, compared with rat cells, human cells in culture are less sensitive to certain AHR agonists and more sensitive to others (Lipp *et al.*, 1992; Nagayama *et al.*, 1985; Silkworth *et al.*, 2005; Zeiger *et al.*, 2001). In particular, a study of freshly isolated human hepatocytes resulted in an ethoxyresorufin-*O*-deethylase (EROD)–based relative potency (REP) value of 0.003 for 3,3',4,4',5-pentachlorobiphenyl (PCB 126), which is 33-fold lower than the current TEF value of 0.1 (Silkworth *et al.*, 2005). This work was recently expanded employing a subset of the same fresh human hepatocytes used by Silkworth *et al.* (2005) to demonstrate that half maximal effective concentration (EC50)–based REP values of PCB 126 for 47 AHR-responsive genes have a geometric mean of 0.002 (Carlson *et al.*, 2009). In contrast, several PCDFs were more potent in human lymphoblastoid cells, as measured by aryl hydrocarbon hydroxylase activity, than would be predicted from their TEF values (Nagayama *et al.*, 1985).

Recent reports (EPA, 2009; NRC, 2007a,b) have endorsed the development of *in vitro* approaches for modern toxicity testing. Such approaches include the improvement of models used to extrapolate across species, the development of a better mechanistic understanding of dose-response, and the development of a more complete understanding of human toxicity pathways. Because it is thought that activation of the AHR is the initial step required (Fernandez-Salguero *et al.*, 1996) for all subsequent toxicity of DLCs and that cytochrome P450 1A1 (*CYP1A1*) messenger RNA (mRNA) induction correlates

© The Author 2010. Published by Oxford University Press on behalf of the Society of Toxicology. All rights reserved.
For permissions, please email: journals.permissions@oxfordjournals.org

well with the potency of DLCs (Poland and Knutson, 1982), AHR-mediated induction of *CYP1A1* gene expression, although not responsible for all DLC toxicities (Uno *et al*., 2004), is a very sensitive, quantitative, and useful indicator of AHR activation.

In order to address these goals and to expand previous observations regarding the potency of DLCs in human cells to an additional cell type, we have studied the induction of *CYP1A1* mRNA in normal human epidermal keratinocytes (NHEKs) exposed to TCDD and several DLCs. NHEKs are responsive to AHR agonists in culture and are highly relevant to the most frequently observed TCDD-mediated toxicity in humans, chloracne (Sutter *et al*., 2009). To test whether differences previously observed *in vitro* between rat and human cell responses extend to this tissue and also apply to additional DLCs, we studied five congeners representing dioxins, furans, and biphenyls. We chose a representative and potent congener from each group: TCDD, 2,3,7,8-tetrachlorodibenzofuran (TCDF), and PCB 126. In addition, 1,2,3,6,7,8-hexachlorodibenzo-*p*-dioxin (HxCDD) was tested because of its prevalence in the environment (Hedgeman *et al*., 2009). To match the chlorination pattern of HxCDD, 1,2,3,6,7,8-hexachlorodibenzofuran (HxCDF) was chosen as a second furan. Each of these chemicals has been assigned a TEF value of 0.1 (Van den Berg *et al*., 2006). Our goal in performing this research was to test whether the assigned TEFs accurately predicted the REPs of these DLCs in a relevant human cell type, thereby providing information that could be used to more closely estimate the risk that exposure to these chemicals may pose to the human population.

MATERIALS AND METHODS

Chemicals. PCB 126 was obtained from Accustandard (New Haven, CT). HxCDD and HxCDF were obtained from Cambridge Isotope Laboratory (Andover, MA). TCDD and TCDF were gifts from W. F. Greenlee (The Hamner Institutes for Health Sciences) and Dow Chemical, respectively. Dimethyl sulfoxide (DMSO) was obtained from Sigma (St Louis, MO).

HRGC/HRMS analysis. Vista Analytical Laboratory performed high resolution gas chromatography/high resolution mass spectroscopy (HRGC/HRMS) analysis of test chemicals using Modified Environmental Protection Agency Methods 8290/1668 to quantify contaminants. The concentration of each of the chemical stock solutions was verified, and contaminants were identified. The purity of each congener was as follows: TCDD, 99.57%; HxCDD, 99.52%; TCDF, 100.0%; HxCDF, 99.62%; and PCB 126, 99.75%. The contaminants altered the toxic equivalence of the chemical being tested by less than 1%. For the TCDD, the only contaminant was 0.43% 1,2,3,7,8-pentachlorodibenzo-*p*-dioxin (PeCDD). For the HxCDD, the two contaminants were 0.38% 1,2,3,4,6,7,8-heptachlorodibenzo-*p*-dioxin and 0.10% 1,2,3,7,8-PeCDD. For HxCDF, the three contaminants were 0.16% 2,3,4,7,8-pentachlorodibenzofuran (PeCDF), 0.15% 1,2,3,7,8-PeCDF, and 0.07% 1,2,3,4,7,8,9,-HpCDF. For PCB 126, the five contaminants were 0.16% PCB 81, 0.04% PCB 77, 0.02% PCB 169, 0.02% PCB 157, and 0.01% PCB 118.

Cell culture. Neonatal foreskin NHEKs, purchased from Lonza (Walkersville, MD), were grown in Keratinocyte-serum-free medium (Invitrogen, Carlsbad, CA). Confluent fifth passage NHEKs were incubated in complete media (50 μg/ml bovine pituitary extract and 5 ng/ml epidermal growth factor [EGF]) for 48 h, changed to basal media (no supplements or serum) for 24 h, and then treated with chemicals in basal media for the time indicated or for 48 h in the dose-response studies (Sutter *et al*., 2009). Rat hepatoblastoma–derived H4IIE American Type Culture Collection cells were grown in Dulbecco's modified Eagle's medium supplemented with 10% fetal bovine serum, 2% L-glutamine, and penicillin/streptomycin. Confluent cells were incubated in basal media (no supplements or serum) for 24 h and then treated with vehicle control (0.7% DMSO) or chemical in basal media for 48 h in triplicate. Serum-free exposure media were used because serum components (e.g., bovine serum albumin) can significantly reduce the cellular uptake of TCDD and DLCs (Hestermann *et al*., 2000). The chemical concentrations tested were the following: TCDD (0.001, 0.01, 0.03, 0.1, 0.3, 1, 3, 10, 30, and 100nM), PCB 126 (0.01, 0.1, 0.3, 1, 3, 10, 30, 100, 300, 1000, 3000, and 10,000nM), or TCDF, HxCDF, and HxCDF (0.01, 0.03, 0.1, 0.3, 1, 3, 10, 30, 100, and 300nM).

Although Rat H4IIE cells are not from the same tissue origin as NHEKs and are thus unable to serve as a direct cell type–specific, interspecies comparison, this sensitive rodent cell line has been previously determined to give replicable DLC REPs consistent with the TEFs. Therefore, we utilized H4IIE cells primarily to validate the bioactivity of low concentrations of our chemical congeners and to check for consistency of rodent-derived REPs under our experimental conditions.

Cell viability assay. Cell viability was measured by a 3-4,5-dimethylthiazol-2-yl)-2,5-diphenyltetrazolium bromide (MTT) assay (Sigma). Cells were treated with vehicle and chemicals for 48 h, after which 75 μl of MTT solution and 750 μl of Hank's balanced salt solution were added to the cells, and plates were incubated for 2 h 30 min at 37°C. The solubilization solution (750 μl) was added to the plates to dissolve the formazan crystals, and the plates were incubated again for another 30 min. Optical density was measured at 570 nm using a spectrophotometer.

Biochemical analyses. Total RNA was isolated using RNA Stat-60 (Tel-Test). Real-time PCR was carried out using the Roche LightCycler 480, LC480 SYBR Green I Master, and the following primers (5′-3′): for human *CYP1A1*, CATCCCCCACAGCACAACAAGAGA and GCAGCAGGATAGCCAG-GAAGAGAA and for rat *Cyp1a1*, CTTCACACTTATCGCTAATGG and TGGGGTCTGAGGCTATGG. Beta actin (*ACTB*) was used as the reference for sample normalization using the following primers: for human *ACTB*, TGGTGGGCATGGGTCAGAAG and GTCCCGGCCAGCCAGGTCCAG and for rat *Actb*, TCCACCCGCGAGTACAACCTTCTT and GGCCCGGG-GAGCATCGTC. The mRNA levels were measured in at least three separate samples for each chemical concentration except in the following cases. Out of the complete data set, there were three samples (donor 1: 3nM TCDF treatment and donor 2: 3nM TCDD and 0.01nM HxCDF treatments) from which RNA values were not obtained and seven samples that were excluded because the values of their *ACTB* mRNA were greater than or equal to the mean *ACTB* level of their respective donor ± 3 SDs (z-ratio ≥ 3). These were from donor 1: 3nM TCDD and 0.01nM HxCDF treatments; donor 2: 30nM TCDD treatment (one of the six samples); donor 3: DMSO treatment (one of nine samples) and 1000nM PCB 126 treatment; and donor 4: 10,000nM PCB 126 treatment.

PCR efficiencies (E) were calculated from the slopes of the standard curves using the equation, $E = 10^{(-1/\text{slope})}$. Standard curves using serial dilutions (NHEK cDNA input of 40–0.0004 ng [$n = 3$]) resulted in a high degree of linearity of *CYP1A1* and *ACTB* mRNA values. The R^2 value for both human *CYP1A1* and human *ACTB* was 0.996. The calculated efficiency, E, for PCR amplification was 1.88 and 1.95 for *CYP1A1* and *ACTB*, respectively. Standard curves using serial dilutions (H4IIE cDNA input of 20–0.00002 ng [$n = 5$]) also resulted in a high degree of linearity of rat *Cyp1a1* and A*ctb* mRNA values. The R^2 value for rat *Cyp1a1* was 1.000 and rat *Actb* was 0.999. The calculated PCR efficiency, E, was 1.94 and 1.98 for rat *Cyp1a1* and rat *Actb*, respectively. Relative quantification of the mRNA was determined using the calculated efficiencies and the previously described method (Pfaffl, 2001). For each NHEK replicate culture, *CYP1A1* expression was normalized relative to the housekeeping gene *ACTB* and also within each donor, relative to the mean *CYP1A1* gene expression level (average of the three replicate cultures) at the TCDD concentration that achieved the highest induction. The resulting normalized data were termed "relative *CYP1A1* expression index." All the experimental values for *CYP1A1* and *ACTB* were in the linear range of each of the standard curves and well within our limits of detection, determined to be at

least twofold lower than the lowest experimental value. When PCR was carried out on samples that did not include reverse transcriptase, the values of *CYP1A1* amplification were 75-fold lower than the lowest experimental value, demonstrating that all our experimental values are far above background levels of *CYP1A1* amplified from contaminating genomic DNA.

Dose-response models for individual donors. A modified version of the Hill equation (Hill, 1910, 1913) was employed for dose-response modeling defined as follows:

$$\mu(\delta) = \frac{\alpha}{1 + 10^{\eta(\pi - \delta)}}, \quad (1)$$

where $\mu(\delta)$ was the estimated mean response (i.e., relative *CYP1A1* expression index) at concentration δ ($\log_{10}$ nanomolar), α the maximal agonist effect (i.e., the change in height of the right asymptote), π the potency ($\log_{10}$ nanomolar) at $\alpha/2$ (i.e., the 50% effective concentration; EC50), and η the Hill coefficient. The baseline expression level at $\delta = -\infty$ was set to be constant at zero, allowing for a more simplified Hill model without constraints. This was a reasonable assumption because the vehicle control expression values did not exceed the 0.01 relative response level (i.e., 1% of the mean maximal *CYP1A1* level for TCDD exposure) for any one cell culture and more complex models not making this assumption did not result in significantly better fits (data not shown). It is important to note that vehicle control data were omitted from the dose-response modeling procedure to avoid $\log_{10}$ transformation of 0nM.

Because the goal of the current study was to accurately estimate DLC REP values, nonlinear dose-response curves were fit simultaneously for TCDD and DLCs using similar procedures to those described previously (Carlson *et al.*, 2009; Toyoshiba *et al.*, 2004). Initially, REP dose-response models were generated separately for each donor-specific data set. To achieve this, the following indicator Equation 2 was employed:

$$\begin{aligned}\pi = {} & \pi_{\mathrm{TCDD}} I_{\mathrm{TCDD}} + (\Delta\pi_{\mathrm{HxCDD}} + \pi_{\mathrm{TCDD}}) I_{\mathrm{HxCDD}} \\ & + (\Delta\pi_{\mathrm{TCDF}} + \pi_{\mathrm{TCDD}}) I_{\mathrm{TCDF}} + (\Delta\pi_{\mathrm{HxCDF}} + \pi_{\mathrm{TCDD}}) I_{\mathrm{HxCDF}} \\ & + (\Delta\pi_{\mathrm{PCB\ 126}} + \pi_{\mathrm{TCDD}}) I_{\mathrm{PCB\ 126}},\end{aligned} \quad (2)$$

where π_{TCDD} was the estimated $\log_{10}$ EC50 for TCDD (i.e., the base chemical) and $\Delta\pi$ was the relative change in $\log_{10}$ EC50 (from TCDD) for the indicated DLC. The indicator functions (I) are equal to 1 when calculating the response of the subscripted chemical; otherwise they are equal to 0. Therefore, if the $\log_{10}$ EC50s for both TCDD and PCB 126 were identical, then the estimated $\Delta\pi_{\mathrm{PCB\ 126}}$ would be equal to 0. Thus, the DLC REP can be easily derived from $\Delta\pi$ using Equation 3.

$$\mathrm{REP}_{\mathrm{DLC}} = 10^{-\Delta\pi}. \quad (3)$$

Because dose-response data for HxCDD and TCDF were only determined for donor 1 NHEKs, Equation 2 for the remaining donors did not include parameters for these congeners.

Although it was expected that each 0.1 TEF DLC congener would act as a full AHR agonist in human keratinocytes to generate parallel dose-response curves of equal maximal agonist effect, preliminary analyses indicated that for some donors the maximal agonist effect (i.e., α) varied significantly among TCDD and DLCs. Therefore, a more complex model was also generated with separate α parameter estimates for each congener (designated by appropriate subscripts). Conversely, an assumption of parallel dose-response curves among congeners appeared legitimate, allowing for the Hill coefficient η to be set not to vary among chemical congeners. Thus, 2 nested models (see below) were attempted for each donor-specific data set.

$$\mu(\delta) = f(\alpha, \pi_{\mathrm{TCDD}}, \Delta\pi_{\mathrm{HxCDD}}, \Delta\pi_{\mathrm{TCDF}}, \Delta\pi_{\mathrm{HxCDF}}, \Delta\pi_{\mathrm{PCB\ 126}}, \delta, \eta) + \varepsilon, (\mathit{Model}\ 1)$$

$$\mu(\delta) = f\begin{pmatrix} \alpha_{\mathrm{TCDD}}, \alpha_{\mathrm{HxCDD}}, \alpha_{\mathrm{TCDF}}, \alpha_{\mathrm{HxCDF}}, \alpha_{\mathrm{PCB\ 126}}, \\ \pi_{\mathrm{TCDD}}, \Delta\pi_{\mathrm{HxCDD}}, \Delta\pi_{\mathrm{TCDF}}, \Delta\pi_{\mathrm{HxCDF}}, \Delta\pi_{\mathrm{PCB\ 126}}, \delta, \eta \end{pmatrix} + \varepsilon. (\mathit{Model}\ 2)$$

A generalized nonlinear least squares procedure (Pinheiro and Bates, 2004) was used to fit each model where parameters in Equation 1 were explained by $f()$, and ε represents the residual error of $\mu(\delta)$ and assumed to be independently distributed as $N\ (0,\sigma^2)$. Again, congener-specific parameters for HxCDD and TCDF were only used for donor 1 NHEK models and omitted for the other donors. The more complex Model 2 was selected over Model 1 only if it was deemed a better fit by likelihood ratio test (LRT, $p \leq 0.05$) and comparison of Akaike information criteria (Akaike, 1974). Because residual analyses indicated significant heteroscedastic residual variance with predicted response for each best-fit dose-response model, a residual variance modeling procedure was employed as previously described (Carlson *et al.*, 2009). In order to generate EC50 maximum likelihood (ML) estimates and approximate 95% confidence intervals (CIs) for each DLC, best-fit models were reparameterized to produce a separate π parameter for each DLC rather than $\Delta\pi$ parameters. In addition, dose-response data for the rat cell line H4IIE were modeled in a manner identical to that described above.

Population-level dose-response model. Following the donor-specific dose-response modeling procedure, data from all donors for the chemical congeners TCDD, HxCDF, and PCB 126 were combined to formulate a "population-level" REP model that would provide model parameter estimates for the average individual in the sampled population. Examination of the donor-specific model outputs revealed that a separate parameter for the maximal agonist effect (α) would likely be required for each chemical congener as done in the donor-specific Model 2. In addition, variability among donors in α_{HxCDF}, $\alpha_{\mathrm{PCB\ 126}}$, and π_{TCDD} would necessitate implementation of a nonlinear mixed-effects model (Lindstrom and Bates, 1990; Pinheiro and Bates, 2004) with random effects allowing these parameters to vary among donors. Furthermore, to permit for subsequent reparameterization of the model to estimate DLC EC50s and approximate 95% CIs, random effects allowing $\Delta\pi_{\mathrm{HxCDF}}$ and $\Delta\pi_{\mathrm{PCB\ 126}}$ to vary among donors were also included in the model. The Hill coefficient η was set to remain constant among chemical congeners (i.e., parallel dose-response curves), as in both Models 1 and 2. Analysis of the donor-specific model output also indicated that the η parameter did not vary much among donors. The full population REP model was defined as follows:

$$\mu(\delta) = f\begin{pmatrix} \alpha_{\mathrm{TCDD}}, \alpha_{\mathrm{HxCDF}} + b_{1i}, \alpha_{\mathrm{PCB\ 126}} + b_{2i}, \\ \pi_{\mathrm{TCDD}} + |b_{3i}, \Delta\pi_{\mathrm{HxCDF}} + b_{4i}, \Delta\pi_{\mathrm{PCB\ 126}} + b_{5i}, \delta, \eta \end{pmatrix} + \varepsilon_i, (\mathit{Model}\ 3)$$

where each parameter in Equation 1 was explained by $f()$ whose arguments included five random effects (i.e., b_{1i}–b_{5i}) representing the variability in the fixed terms α_{HxCDF}, $\alpha_{\mathrm{PCB\ 126}}$, π_{TCDD}, $\Delta\pi_{\mathrm{HxCDF}}$, and $\Delta\pi_{\mathrm{PCB\ 126}}$, respectively, among the donors i. The value of index i ranged from 1 to 4 (i.e., the four human donors). All random effects in Model 3 were assumed to be normally distributed with mean 0 and variance-covariance matrix $\boldsymbol{\psi}$ (i.e., a general positive-definite matrix) independently for each donor i. The residual error ε_i was assumed to be independently distributed as $N\ (0,\sigma^2)$ and independent of any random effects.

Threshold model. A population-level "hockey stick" model was generated to estimate TCDD, HxCDF, and PCB 126 potencies at dose-response thresholds in the low-dose region using piecewise regression procedure similar to those described elsewhere (Bacon and Watts, 1971; Lutz and Lutz, 2009; Seber and Wild, 2003; Yanagimoto and Yamamoto, 1979). Arguably, the best scale in which to define a threshold response would be in log-log space, where both the response and concentration are $\log_{10}$ transformed (Bailey *et al.*, 2009a,b; Slob, 2007; Williams *et al.*, 2009), thereby accentuating very small changes in gene expression at low exposure levels. Thus, both concentration and response were $\log_{10}$ transformed prior to dose-response modeling for this procedure. Data at the high concentration end (i.e., right asymptote) of sigmoid curves of each chemical were subsequently removed in a nonbiased manner to generate hockey stick dose-response shapes as they did not inform the dose-response at lower response points (see Supplementary methods section). The piecewise equation was defined as follows:

$$\mu(\delta) = \begin{Bmatrix} \alpha_0 & \text{for } \delta \leq \tau \\ \alpha_0 + \beta(\delta - \tau) & \text{for } \delta > \tau \end{Bmatrix}, \quad (4)$$

where $\mu(\delta)$ was the $\log_{10}$-transformed mean response at concentration δ ($\log_{10}$ nanomolar), α_0 the baseline expression level at $\delta = -\infty$, τ the break point

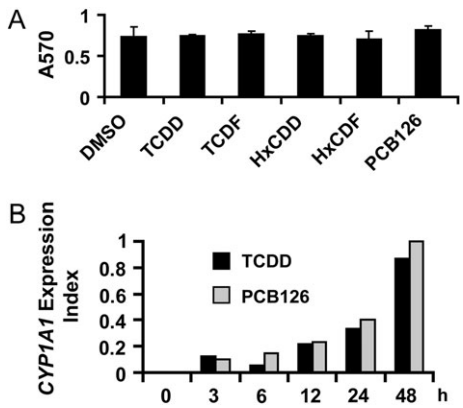

FIG. 1. (A) NHEKs were treated with control vehicle (DMSO, 0.7%), TCDD (100nM), TCDF (300nM), HxCDD (300nM), HxCDF (300nM), or PCB 126 (10,000nM) for 48 h. Cell viability was determined using the MTT assay as described in Materials and Methods section, which measures absorbance at 570nM. The results are presented as mean ± SD ($n = 3$). (B) NHEKs were treated with TCDD (10nM) or PCB 126 (10,000nM) for 0, 3, 6, 12, 24, and 48 h. Real-time PCR was used to determine the level of *CYP1A1* mRNA. Levels of mRNA are expressed in units relative to the maximum, given a value of 1.

(i.e., threshold) concentration, and β the slope of the dose-response above τ. It is important to note that this equation is continuous at $\delta = \tau$, where a flat line with slope zero and y-intercept α_0 intersects a second line with slope β.

A nonlinear modeling procedure was employed to allow for direct estimation of threshold locations (Seber and Wild, 2003). All three chemical congeners were modeled simultaneously, as was done with Models 1–3, but instead of estimating REP values for HxCDF and PCB 126 at the EC50 level, the REP values were determined at the threshold concentration τ level. Therefore, we defined this new "low-dose" REP as the relative threshold factor (RTF). An indicator equation similar to Equation 2 was generated, where τ_{TCDD} was the estimated threshold concentration for TCDD and $\Delta\tau_{HxCDF}$ and $\Delta\tau_{PCB\ 126}$ were the relative changes in the threshold concentration for HxCDF and PCB 126, respectively. By replacing Δπ with Δτ in Equation 3, the RTF for each DLC can be derived. The final nonlinear mixed-effects model was defined as follows:

$$\mu(\delta) = f(\alpha_0 + b_{1i}, \tau_{TCDD}, \Delta\tau_{HxCDF}, \Delta\tau_{PCB\ 126}, \delta, \beta + b_{2i}) + \varepsilon_i, (Model\ 4)$$

where each parameter in Equation 4 was explained by *f*() whose arguments included 2 random effects (i.e., b_{1i} and b_{2i}) representing the variability in the fixed terms α_0 and β, respectively, among the donors *i*. The value of index *i* ranged from 1 to 4 (i.e., the four human donors). Random effects in Model 4 were assumed to be normally distributed with mean 0 and variance-covariance matrix (i.e., a general positive-definite matrix) independently for each donor *i*. The residual error ε_i was assumed to be independently distributed as $N(0,\sigma^2)$ and independent of any random effects.

Statistical functions. The "gnls" function in the R package nlme version 3.1-96 (Pinheiro and Bates, 2004) was used to fit Models 1 and 2 and the function "nlme" from the same package was used for Models 3 and 4. The "method" argument for Models 3 and 4 was set to "ML" or maximized log likelihood. All functions were implemented in *R* version 2.10.1 (R Development Core Team, 2006). The starting value selection procedure employed for each model is described in detail in the Supplementary methods section. A semiparametric (residual based) bootstrap method (10,000 resamplings) was employed to approximate 95% CIs for chemical-specific threshold models in a manner identical to that previously described by Toms and Lesperance (2003).

RESULTS

Characterization of Test Chemical Treatments

TCDD-mediated increases in *CYP1A1* mRNA in donor 1 NHEKs have been previously demonstrated to be greatest in confluent cultures in which EGF was omitted (Sutter *et al.*, 2009). Cell culture conditions in the studies presented here are similar to those previously described to ensure maximal responsiveness of *CYP1A1* mRNA. MTT cell–based viability assay in NHEKs indicated that at the maximum concentration used in these studies, none of the chemicals caused cell toxicity (Fig. 1A), consistent with previous results using TCDD in numerous cultures of cells (Knutson and Poland, 1980). A time-course study measuring *CYP1A1* mRNA in NHEKs (Fig. 1B) indicated that TCDD (10nM) had a response that was parallel and similar in magnitude to PCB 126 (10,000nM). These concentrations were selected based on the study of Silkworth *et al.* (2005). Because these responses continued to increase up to 48 h and for consistency with the exposure duration of previous dose-response studies conducted in our laboratory using fresh human and rat hepatocytes (Carlson *et al.*, 2009; Silkworth *et al.*, 2005), this time of exposure was chosen for the dose-response studies and longer exposure durations were not analyzed.

Dose-Response for Individual Donors

NHEKs from four donors were used to study the *CYP1A1* mRNA concentration-response. Initially, dose-response was determined for TCDD and four DLCs with assigned TEFs of 0.1 (i.e., HxCDD, TCDF, HxCDF, and PCB 126) in only donor 1 NHEKs. Because both HxCDD and TCDF appeared to produce the expected REP of 0.1 for donor 1 NHEKs, only TCDD, HxCDF, and PCB 126 were tested in NHEKs from donors 2–4.

Donor-specific REP models were initially generated separately for NHEKs from each of the four donors, and model output data are given in Table 1 and presented graphically in Figure 2. The more complex Model 2, with separate maximal agonist effect parameters (i.e., α) for each chemical, was selected for donors 1, 3, and 4 by a log LRT ($p \leq 0.05$), whereas the more parsimonious Model 1 (i.e., same α for all congeners) was selected for donor 2 NHEKs ($p = 0.4974$). Model residual variance was seen to increase with increasing fitted values (i.e., heteroscedastic residual variance) for all donor-specific REP models, necessitating residual variance modeling procedures which greatly improved residual variance homogeneity.

As indicated earlier, the estimated REP values for HxCDD (0.24) and TCDF (0.10) for donor 1 NHEKs were within the half order of magnitude uncertainty prescribed to their assigned TEFs of 0.1 (Van den Berg *et al.*, 2006), whereas considerable deviations for estimated REP values of HxCDF (1.1) and PCB 126 (0.003) from their TEFs of 0.1 were determined (Table 1). Consistent with the donor 1 model, dose-responses for donors

TABLE 1
Donor-Specific REP Model Outputs

Chemical	Culture	Maximal agonist effect[a]	Hill coefficient	EC50 (nM)	REP	WHO TEF[b]
TCDD	Donor 1	0.98 (0.90–1.06)[c]	1.4 (1.3–1.6)	0.56 (0.43–0.72)	1	1
	Donor 2	0.92 (0.88–0.95)	1.3 (1.2–1.5)	0.32 (0.26–0.39)	1	1
	Donor 3	0.94 (0.85–1.03)	1.4 (1.1–1.6)	0.45 (0.33–0.62)	1	1
	Donor 4	0.91 (0.76–1.06)	1.1 (0.9–1.3)	1.41 (0.82–2.43)	1	1
HxCDD	Donor 1	1.19 (1.11–1.28)	1.4 (1.3–1.6)	2.32 (1.85–2.91)	0.24 (0.17–0.33)	0.1
TCDF	Donor 1	0.89 (0.81–0.98)	1.4 (1.3–1.6)	5.44 (4.02–7.35)	0.10 (0.07–0.15)	0.1
HxCDF	Donor 1	0.91 (0.85–0.98)	1.4 (1.3–1.6)	0.53 (0.41–0.68)	1.06 (0.75–1.49)	0.1
	Donor 2	0.92 (0.88–0.95)	1.3 (1.2–1.5)	0.39 (0.30–0.51)	0.82 (0.61–1.10)	0.1
	Donor 3	0.72 (0.65–0.79)	1.4 (1.1–1.6)	0.99 (0.69–1.42)	0.45 (0.29–0.70)	0.1
	Donor 4	0.59 (0.50–0.68)	1.1 (0.9–1.3)	0.65 (0.37–1.16)	2.16 (1.09–4.30)	0.1
PCB 126	Donor 1	0.92 (0.83–1.01)	1.4 (1.3–1.6)	188.58 (143.81–247.28)	0.0030 (0.0021–0.0042)	0.1
	Donor 2	0.92 (0.88–0.95)	1.3 (1.2–1.5)	204.12 (157.08–265.25)	0.0016 (0.0012–0.0021)	0.1
	Donor 3	0.32 (0.25–0.38)	1.4 (1.1–1.6)	156.08 (87.51–278.38)	0.0029 (0.0015–0.0054)	0.1
	Donor 4	0.51 (0.36–0.65)	1.1 (0.9–1.3)	377.39 (176.08–808.86)	0.0037 (0.0017–0.0084)	0.1

[a]Response units are relative *CYP1A1* expression index as described in the Materials and Methods section.
[b]Van den Berg *et al.* (2006).
[c]All data are expressed as ML estimate and 95% CI (in parentheses).

2–4 revealed relatively higher HxCDF and lower PCB 126 REP estimates than the assigned TEF of 0.1. Model estimates for the Hill coefficient were similar across the donors, whereas the TCDD EC50 for donor 4 NHEKs was relatively higher than estimates for the other three donors. The maximal agonist effects elicited by PCB 126 and HxCDF in NHEKs from donors 3 and 4, but not donors 1 and 2, were clearly lower than that observed for TCDD (Fig. 2), indicating that these congeners may not always act as full agonists of the AHR in NHEKs.

Population Dose-Response

Observations made from the donor-specific modeling procedure were used to formulate a population-level REP model that simultaneously fit dose-response data for TCDD, HxCDF, and PCB 126 from all donor NHEK cultures. Because we were interested in parameter estimates representing the average individual of our "population" and the approximate 95% CIs surrounding each parameter, a mixed-effects modeling procedure was implemented. Donor-specific data given in Table 1 suggested that random effects accounting for donor-to-donor variability in EC50s (and REP values) and the maximal agonist effect for both HxCDF and PCB 126 might be necessary. These assumptions were justified by log-likelihood ratio testing among various population REP models when donor-specific data were combined (data not shown). Residual variance of the final population REP model was heteroscedastic with increasing fitted values, but implementation of several residual variance modeling procedures failed to generate any convergent models. The final population REP model output data are given in Table 2, and the population-level predicted values are plotted in Figure 3. For comparative purposes and to validate previous observations using our current experimental protocols, dose-response data from the rat hepatoma cell line H4IIE, modeled in a manner identical to that used for NHEK donor–specific modeling, are also depicted in Table 2 and Figure 3. Consistent with the donor-specific models, the NHEK population REP model estimated relatively higher HxCDF and lower PCB 126 REPs than the assigned TEF of 0.1 (Table 2). In addition, the estimated population-level maximal agonist effect for PCB 126 (i.e., α_{PCB126}) was relatively lower than those of TCDD and HxCDF, indicating that PCB 126 may not always act as a full AHR agonist in NHEKs. In stark contrast to these observations, the rat H4IIE cell line model estimated REP values for HxCDF (0.088) and PCB 126 (0.082) that are close to their assigned TEF of 0.1. The estimated TCDD EC50 for H4IIE cells was similar to the ~0.01nM TCDD EC50 value previously reported for H4IIE cells by Peters *et al.* (2004). Figure 3 clearly demonstrates approximately 725-fold lower sensitivity of NHEKs to PCB 126 than the rat H4IIE cell line. This species difference in responsiveness to PCB 126 is well beyond the approximate 23-fold difference seen between TCDD EC50s from the two species and similar to that previously observed for EROD induction in fresh human and rat hepatocytes (Carlson *et al.*, 2009; Silkworth *et al.*, 2005). Interestingly, cells from both species appeared to be nearly equally responsive (i.e., approximately twofold difference) to HxCDF (Table 2).

Calculation of a Population Threshold

Although the nonlinear mixed-effects procedure employed to generate a population REP model appeared to accurately account for the large variability seen among donors in maximal agonist effect, the resulting model was very complex and its

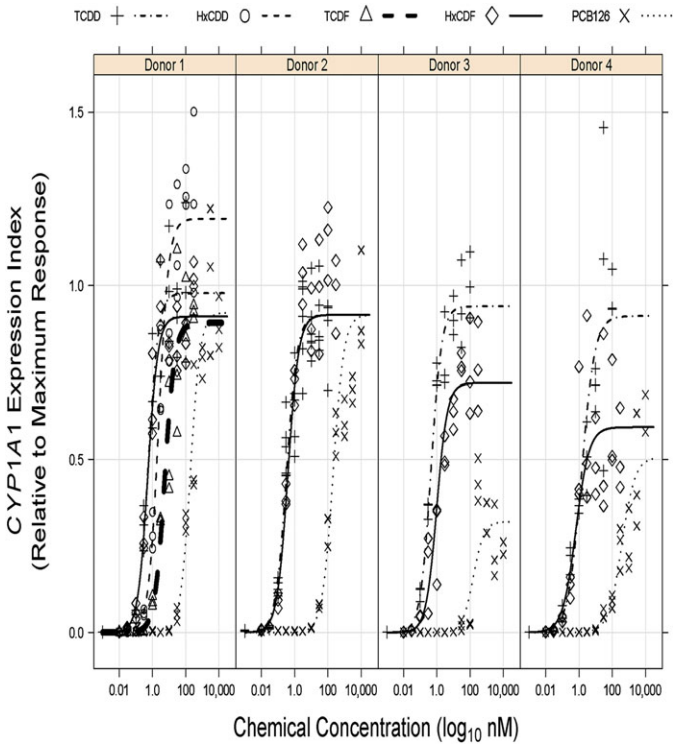

FIG. 2. *CYP1A1* mRNA increases in NHEKs from four donors treated with DLCs modeled as individual donors. NHEKs from donor 1 were treated with DMSO (0.7%) or increasing concentrations of TCDD, TCDF, HxCDD, HxCDF, or PCB 126 for 48 h (see Materials and Methods section for concentrations). NHEKs from donors 2–4 were treated with DMSO (0.7%) or increasing concentrations of TCDD, HxCDF, or PCB 126 for 48 h. The individual culture data points were graphed relative to the average maximum TCDD response reached by each individual donor. Curves represent predicted responses generated by the models described in the Materials and Methods section.

TABLE 2
"Population-Level" REP Model Outputs

Model parameter	NHEK cell population model	Rat H4IIE cell line model[a]
Maximal agonist effect[b]		
TCDD	0.93 (0.90–0.96)[c]	0.93 (0.88–0.98)
HxCDF	0.81 (0.65–0.98)	0.82 (0.77–0.88)
PCB 126	0.65 (0.41–0.89)	0.91 (0.86–0.96)
Hill coefficient	1.2 (1.1–1.4)	1.1 (1.1–1.2)
EC50 (nM)		
TCDD	0.60 (0.31–1.19)	0.026 (0.020–0.032)
HxCDF	0.62 (0.38–1.01)	0.29 (0.23–0.36)
PCB 126	224.73 (115.08–439.86)	0.31 (0.25–0.39)
REP		
HxCDF[d]	0.98 (0.38–2.52)	0.088 (0.067–0.115)
PCB 126[d]	0.0027 (0.0018–0.0039)	0.082 (0.062–0.108)

[a]Although not derived from the same cell type as NHEKs, model output data for rat line H4IIE cell line are given to reiterate previously determined responses of a sensitive rodent cell type under current experimental conditions.
[b]Response units are as described for relative *CYP1A1* expression index in the Materials and Methods section.
[c]All data are expressed as ML estimate and 95% CI (in parentheses).
[d]Current WHO TEF is 0.1 (Van den Berg *et al.*, 2006).

residual variance increased with increasing predicted response level. Since accurate estimation of both EC50s and EC50-derived REP values depend upon precise determination of the right asymptote of the sigmoid dose-response curve (i.e., maximal agonist effect), we sought to take advantage of the strikingly similar response among donors apparent at lower chemical concentrations (as observed in Fig. 3) to develop an alternative method to assess potency and REP using our data. To achieve this, a population threshold model, resembling a hockey stick in shape, was developed where the initial dose-response relationship is flat across chemical concentrations (zero slope) followed by a concentration-dependent, linearly increasing response beyond an unknown threshold. This model directly estimated the TCDD threshold concentration (i.e., τ_{TCDD}) and RTFs for HxCDF and PCB 126. Residual variance of the final threshold model was homogeneous across all response levels (i.e., the assumption that residuals were independent and identically distributed was justified).

The population threshold model output data are given in Table 3, and Figure 4 depicts the predicted population-level response obtained for each chemical. For entirely informational purposes, relative *CYP1A1* expression indices of the vehicle control samples used in this study are also included in Figure 4, although vehicle control data were not used in the actual threshold modeling. A more complex model allowing the slope of the initial line segment below the threshold to deviate from zero (i.e., a concentration-effect below threshold) did not prove a better fit by log LRT ($p = 0.7018$). Overall, the RTFs generated in the population threshold modeling procedure (Table 3) were entirely consistent with REP values derived from full dose-responses shown in Table 2, demonstrating that the clear divergence of HxCDF and PCB 126 NHEK-derived REP values from their assigned TEFs also occurs in the low concentration-effect region.

Our analyses to validate our methods for relative quantitative real-time PCR (see Materials and Methods section) demonstrated that we were able to accurately detect low levels of *CYP1A1* mRNA transcripts in the control samples and the samples below the apparent threshold concentrations. In addition, increases in *Cyp1a1* mRNA in H4IIE cells were detected by exposure to low concentrations of chemicals, although they did not elicit a response in NHEKs, demonstrating that the chemicals are biologically available at these lower concentrations (Fig. 3).

Several mathematical caveats are always associated with threshold modeling, including convergence problems because of log-likelihood surfaces with multiple local maxima/flat ridges and the possibility of discontinuous first derivatives (Bacon and Watts, 1971; Seber and Wild, 2003). For

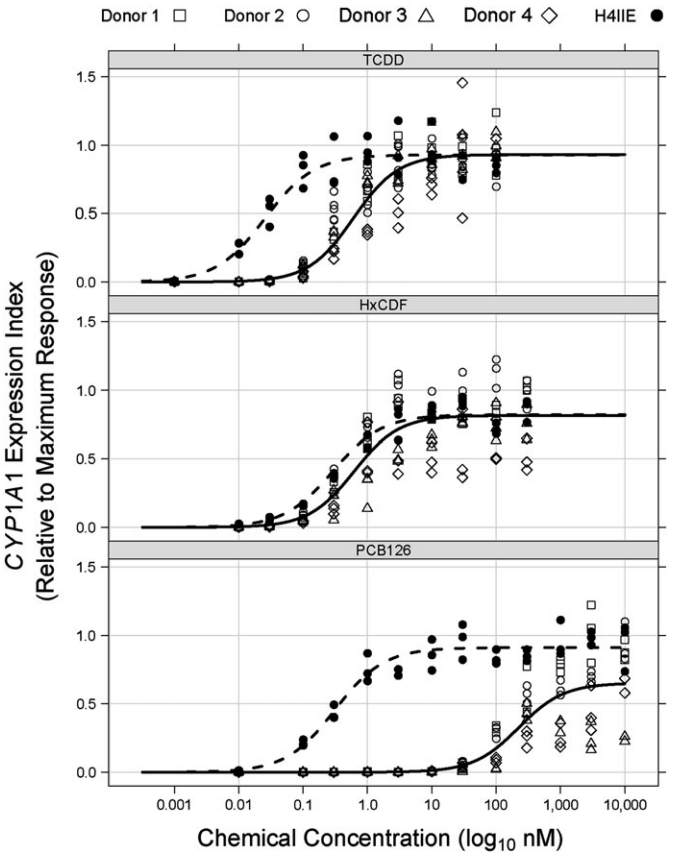

FIG. 3. *CYP1A1* mRNA increases in NHEKs from four donors treated with TCDD, HxCDF, and PCB 126 modeled together as a population and compared with the rat liver cell line H4IIE. Relative *CYP1A1* levels from NHEKs from each donor and from H4IIE cells after 48 h treatment with TCDD (upper panel), HxCDF (middle panel), and PCB 126 (lower panel) are plotted as indicated. Each point in the graphs represents an individual sample. Data were modeled as described in the Materials and Methods section, resulting in a population-level prediction curve for NHEKs (solid line) and the predicted response of rat H4IIE cells (dashed line).

a nonlinear piecewise model such as the one employed in the current study, careful attention needs to be paid to the choice of starting values for threshold parameters (Brenden and Bence, 2008). We conducted a grid search (Lerman, 1980) of "residual sum of squares" profiles using simple linear models to generate optimal starting values for threshold concentrations and RTFs. In addition, the stability of parameter estimates of the final threshold model was verified by varying threshold starting values in 0.2nM increments throughout the concentration ranges. Finally, examination of the log-likelihood surfaces for various parameter combinations in the population threshold model did not reveal the possibility of local maxima (data not shown).

Another problem commonly encountered in piecewise regression is that the assumption of asymptotic normality for the threshold parameter distribution might not be always justified (Feder, 1975a,b; Hinkley, 1969, 1971), making the

TABLE 3
Threshold Model Outputs

Model parameter	Estimate
Baseline response level[a]	1×10^{-3} (7×10^{-4} to 3×10^{-3})[b]
Threshold concentration (nM)	
TCDD	0.0062 (0.0052–0.0073)
HxCDF	0.0067 (0.0056–0.0079)
PCB 126	2.8 (2.4–3.3)
RTF[c]	
HxCDF[d]	0.93 (0.81–1.07)
PCB 126[d]	0.0022 (0.0019–0.0025)
Slope below threshold[e]	0
Slope above threshold	1.27 (1.17–1.37)

[a]Response units are relative *CYP1A1* expression index.
[b]All data are expressed as ML estimate and 95% CI (in parentheses).
[c]REP derived with threshold concentrations instead of EC50s.
[d]Current WHO TEF is 0.1 (Van den Berg *et al.*, 2006).
[e]This model parameter is forced to equal zero.

ML approximation method for derivation of asymptotic CIs in the nlme function (Lindstrom and Bates, 1990) potentially unreliable. Generally, investigators will attempt various alternative methods to estimate threshold uncertainty such as inversion of the *F* statistic and/or bootstrapping (Toms and Lesperance, 2003); however, such analyses using our threshold model are somewhat impeded because of inherent difficulty in how to fix some parameters and not others and a lack of resampling methods for multilevel mixed-effects models.

Nonetheless, we did attempt to address these issues. Less complex threshold models were generated separately for each chemical congener, without random effects, and 95% CIs were approximated using a semiparametric (residual based) bootstrapping method (first row in Table 4). Using this strategy, we were unable to obtain a convergent model for HxCDF, primarily because of a lack of information regarding the location of the baseline expression level α_0. Next, chemical-specific mixed-effects models were generated with random effects for baseline expression α_0 and slope after threshold β parameters among donor cultures (second row of Table 4). Although we still could not model HxCDF, relatively narrower approximated 95% CIs were estimated for both TCDD and PCB 126 models. It is important to note that the 95% CIs for these chemical-specific mixed-effects models were derived using the nlme ML approximation method, which assumed asymptotic normality. Finally, all three congeners were modeled simultaneously, as was done in Model 4, but the assumption of parallel slopes (i.e., β parameter) among the congeners was not made (third row of Table 4). By borrowing information regarding the baseline expression level across chemicals, the HxCDF dose-response could now be modeled. It is also evident that our previous assumption regarding the existence of parallel dose-responses among chemicals after the threshold (model in the fourth row of Table 4) clearly did not

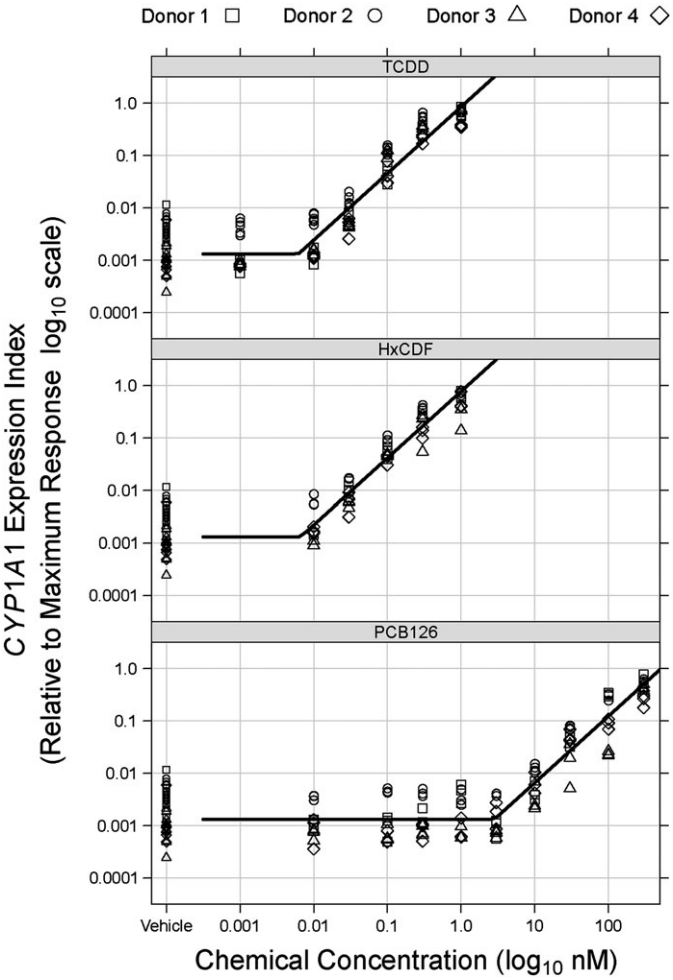

FIG. 4. Models of apparent population thresholds for NHEKs treated with TCDD, HxCDF, and PCB 126. Relative *CYP1A1* mRNA increases from each of the four donors treated with TCDD (upper panel), HxCDF (middle panel), and PCB 126 (lower panel) were plotted and analyzed as described in Materials and Methods section. Each point in the graphs represents an individual sample, and curves are the population-level response predicted by the threshold model. Note that both axes are $\log_{10}$ transformed.

affect the estimation of threshold concentrations to any extent. Thus, the final implementation of a nonlinear mixed-effects threshold model allowed for robust estimation of threshold locations of all three congeners by accounting for donor-to-donor variability in model parameters and "borrowing" information across chemicals, resulting in threshold and RTF estimates with relatively narrow approximated 95% CIs.

DISCUSSION

The concept of TEFs, where DLCs are ranked relative to the potency of TCDD, was developed as a means to quantify exposure to DLCs through dietary intake (Van den Berg *et al.*, 2006). Because TEFs are designed to reflect both pharmacokinetic and pharmacodynamic aspects of DLC toxicity, the TEF committee has given REPs derived from *in vivo* rodent feeding studies more weight than those determined using *in vitro* cell culture techniques. Nonetheless, this expert panel did realize the potential utility of *in vitro* REPs, particularly in characterizing the potency of DLCs lacking any reliable *in vivo* data (Van den Berg *et al.*, 2006). In fact, *in vitro* REPs exist for most DLCs possessing TEFs in the Haws *et al.* (2006) database, with some congeners entirely lacking *in vivo*–derived REPs (e.g., HxCDD). Further examination of the Haws *et al.* (2006) database has revealed a relatively high concordance among *in vitro* and *in vivo* REPs for at least some DLCs. For example, the 50th percentile *in vitro* and *in vivo* REPs for HxCDF (also used in the current study) are 0.063 and 0.081, respectively (Haws *et al.*, 2006). Interestingly, the 50th percentile of PCB 126 REPs derived from *in vitro* studies (i.e., 0.05) was a half order of magnitude lower than that for *in vivo* studies (i.e., 0.1), primarily because of the inclusion of eight relatively lower REP estimates derived from four studies using human cell lines whose geometric mean REP was 0.007 compared with a geometric mean of 0.1 for 21 nonhuman cell–derived REPs (Haws *et al.*, 2006). Overall, such *in vitro* to *in vivo* comparisons using rodent data could potentially be combined with *in vitro* REP estimates generated using human cells to begin to address the cross-species extrapolation of TEF values from rodents to humans using a "parallelogram" approach similar to that previously described by Sobels (1980). However, caution should be given regarding *in vitro* to *in vivo* extrapolations for DLCs whose pharmacokinetics might vary significantly from that of TCDD (e.g., 2,3,4,7,8-PeCDF; Budinsky *et al.*, 2006).

It is generally accepted that the AHR mediates most, if not all, of the toxic responses associated with dioxin exposure. Although not responsible for all toxicities related to AHR activation, CYP1A1 induction represents an endpoint that remains a sensitive indicator of the potency of a DLC to elicit a toxicological response. As activation of the AHR is clearly accepted as an early key event in the mode of action of DLCs, human *in vitro* studies, which measure this activation, provide information more relevant to humans, as well as decrease the use of laboratory animals. Relevancy to humans as well as reducing animal use are recognized by the National Research Council as important goals of future toxicological testing for determination of human health risk (NRC, 2007b). The application of the *in vitro*–derived human potency factors for DLCs is a prime example that embraces this vision.

A number of *in vitro* studies indicate that potency of DLCs, as measured by CYP1A1 induction, differ between rodent and human cells (Carlson *et al.*, 2009; Nagayama *et al.*, 1985; Silkworth *et al.*, 2005; Westerink *et al.*, 2008; Zeiger *et al.*, 2001). To expand on these previous observations, we compared the concentration-dependent induction of *CYP1A1* mRNA in NHEKs treated with TCDD to the concentration-dependent induction of *CYP1A1* mRNA by treatment with four other DLCs. The chosen compounds, HxCDD, TCDF,

TABLE 4
Effects of Various Approaches/Assumptions on Threshold Dose-Response Modeling

Model	Threshold concentration (nM)		
	TCDD	HxCDF	PCB 126
Chemical specific[a]	0.0067 (0.0046–0.0094)[b]	DNC[c]	2.7 (1.9–4.2)
Chemical specific with random effects[d]	0.0067 (0.0052–0.0086)	DNC	2.7 (2.2–3.4)
Multi-chem with random effects[e]	0.0068 (0.0057–0.0083)	0.0060 (0.0048–0.0075)	2.7 (2.2–3.3)
Multi-chem with random effects and parallel slope[f]	0.0062 (0.0052–0.0073)	0.0067 (0.0056–0.0079)	2.8 (2.4–3.3)

[a]Single chemical nonlinear least squares models without random effects; 95% CIs were estimated using semiparametric (residual) bootstrapping (see Materials and Methods section).

[b]All data are expressed as ML estimate and 95% CI (in parentheses).

[c]Did not result in a convergent model.

[d]Single chemical nonlinear mixed-effects models with random effects allowing the baseline expression level and slope after the threshold to vary among donors. The asymptotic 95% CIs for this model were derived using the nlme function.

[e]Nonlinear mixed-effects model using data from all three chemical congeners with random effects allowing for baseline expression level and slope after threshold to vary among donors. The slope after threshold was not assumed to be parallel among the chemicals. The asymptotic 95% CIs for this model were derived using the nlme function.

[f]Same ''population-level'' threshold model described in Table 3 and Figure 4. This model assumed parallel slopes across chemicals, an important assumption of the current TEF approach (Van den Berg *et al.*, 2006).

HxCDF, and PCB 126, representing three different classes of congeners, dioxins, furans, and biphenyls, each had a TEF of 0.1. The initial study (NHEKs from donor 1) indicated that the REP values for HxCDD and TCDF were similar to their TEF values of 0.1 and these congeners were not further analyzed; yet, the REP values for HxCDF and PCB 126 differed from their assigned TEF. A population analysis of NHEKs from four donors indicated that the REP value for PCB 126 was 37.0 times lower and for HxCDF was 9.8 times higher than their TEF values. This indicates that NHEKs are less sensitive to PCB 126 but more sensitive to HxCDF than would be predicted by their assigned TEF values and that the TEF values of HxCDD and TCDF accurately predict the *in vitro* human response compared with TCDD. Because some, but not all, REP values of dioxins and furans deviated from their assigned TEF of 0.1, the results do not support a generalization for all congeners with a similar chlorination patterns. In addition, our results indicate that the differences between *in vitro* human and rodent responses may be congener specific and reiterate that the current TEF values do not always accurately predict the response of human cells to DLCs.

In the current study, we also present a threshold dose-response model used to determine RTFs for HxCDF and PCB 126 in the low concentration region. We fully appreciate the controversy surrounding the existence/absence of dose-response thresholds within the realm of toxicology and have no intention to add fuel to a topic that will be argued *ad infinitum*. Our threshold dose-response model was generated with a clear purpose in mind, to better estimate the REPs of DLCs from an *in vitro* assay system. Residuals of the population-level REP model, using the full dose-response for each chemical, were heteroscedastic largely because of huge variability in response at higher chemical concentrations both between NHEK donors and within replicate cultures. Furthermore, PCB 126 and, to a lesser extent, HxCDF appeared to act as partial AHR agonists in some NHEK donors. Similar problems were also apparent in a previous study using fresh human hepatocytes (Carlson *et al.*, 2009) and will likely be encountered with greater frequency with increased use of untransformed human cell cultures. These aforementioned observations put into question REP values derived by comparing EC50s as suggested by Van den Berg *et al.* (2006) because EC50s rely mainly upon accurate estimation of the maximal agonist effect (right asymptote), and REP values additionally assume that DLCs act as full AHR agonists to generate maximal responses equal to that of TCDD.

Therefore, we took advantage of the strikingly consistent dose-response observed at lower concentrations, which demonstrated a clear break point in *CYP1A1* expression from a relatively flat baseline level to a somewhat monotonically increasing induction. The resulting threshold model estimated RTF values very close to the EC50-based REP values. This concordance indicates that RTFs could function not only in support of EC50-based REP values but also possibly substitute for REP values when a maximum response cannot be accurately determined. However, as noted by others (Howard *et al.*, 2010; Sutter *et al.*, 2006), REP values (and likewise RTFs) would not accurately predict responses of partial agonists at high doses, although the relevancy of potency differences at very high doses to endpoints of interest may be dubious. Furthermore, if the most potent dioxin-like PCB congener (i.e., PCB 126) does not always act as a full AHR agonist in human cells, then application of the TEF scheme to mixtures containing other less potent dioxin-like PCBs, previously demonstrated to act as very weak agonists or

display no activity at all in human cells (Vamvakas *et al.*, 1996; Westerink *et al.*, 2008; Zeiger *et al.*, 2001), will certainly overpredict toxicity.

The apparent threshold for *CYP1A1* induction observed in the current study is entirely consistent with previous observations of a switch-like mechanism of CYP1A1 induction, where within a single cell CYP1A1 is either at a low constitutive expression level or fully induced upon chemical exposure and induction magnitude varies from cell to cell even for the H4IIE cell line (reviewed by Wilson, 2004). This switch-like *CYP1a1* response has been demonstrated in rodent hepatocytes *in vitro* and in the rat liver *in vivo* in response to TCDD and PCB 126 (Bars and Elcombe, 1991; Broccardo *et al.*, 2004, 2005; French *et al.*, 2004; Tritscher *et al.*, 1992). Such switch-like gene regulatory systems have been described elsewhere and are prevalent in biological systems (Ertel and Tozeren, 2008; Lipshtat *et al.*, 2010). We believe that the threshold concentrations determined in the current study, particularly for PCB 126, are not technical artifacts. The subthreshold concentrations of PCB 126 had biological activity in rat H4IIE cells. Also, *CYP1A1* expression levels in the vehicle control and subthreshold concentration exposure groups were well above the background noise of the assay (see Materials and Methods section). Linear mixed-effects regression of PCB 126 data (untransformed) from 0 to 3nM (i.e., within the threshold concentration 95% CI) did not have a positive slope and was not significantly different from a flat zero slope line (data not shown). Because of the extremely high sensitivity of the real-time PCR assay employed, it is conceivable that below the threshold concentration, no or very few NHEKs were switched "on," although we did not look at expression on a cell-by-cell basis.

This study in NHEKs investigated the response of a single gene, *CYP1A1*, to exposure to DLCs, which arguably resulted in a gene-specific REP or RTF. Such "functional selectivity" has been observed for certain receptor ligands where variation exists among REPs across different cellular responses (Kenakin, 2007; Michel and Alewijnse, 2007; Urban *et al.*, 2007). However, a previous toxicogenomic study using fresh human and rat hepatocytes exposed to TCDD or PCB 126 *in vitro* demonstrated a relative consistency of EC50-derived PCB 126 REP estimates across different genes and functional gene categories, indicating that TEFs might be endpoint invariant, at least within this specific cell type (Carlson *et al.*, 2009). It would be of interest to conduct a similar toxicogenomic examination of additional AHR-regulated genes in human keratinocytes in the future, specifically using the novel RTF approach employed in the current study.

The reasons for the large discrepancies between rodent and human *in vitro* concentration-responses to DLCs, as observed previously and in the current study, are not readily apparent. When receptor affinity is considered, it is clear that the AHR in the sensitive mouse strain, AhR b-1, has a 10-fold higher affinity for TCDD (Ema *et al.*, 1994; Harper *et al.*, 1988) than the human AHR because of an amino acid substitution at amino acid 381 in human receptor (Ramadoss and Perdew, 2004) and that the rat AHR has an approximately twofold higher affinity for TCDD than human AHR (Fan *et al.*, 2009). Interestingly, the relative (to TCDD) rat and human AHR affinities for a number of DLCs, including PCB 126, were found to be similar (Fan *et al.*, 2009), indicating that receptor affinity accounts for a nonspecific decrease in sensitivity for most if not all DLCs in human cells compared with rodent cells but cannot explain why human cells are much less sensitive to a DLC such as PCB 126 or more sensitive to one such as HxCDF than the rodent-based TEF would predict. In addition to the general 10-fold decrease in human sensitivity, the NHEK-derived REP for *CYP1A1* induction calculated here for PCB 126 is 26–55 times lower than its TEF of 0.1 and for HxCDF approximately 4–10 times greater, indicating that there are other factors besides the affinity for the AHR that determine sensitivity. It has been suggested that ligand-specific coactivator or corepressor recruitment, that is also dependent upon the species, is likely to determine the sensitivity of a species to DLCs (Flaveny *et al.*, 2008; Zhang *et al.*, 2008). One study using a two-hybrid assay suggests that utilization of certain coactivators by the AHR is dependent on the binding of specific AHR ligands as well as cell context (Zhang *et al.*, 2008); another demonstrates that human and mouse AHRs differ in their ability to interact with coactivators containing LXXLL motifs, suggesting differential recruitment of coactivators between mouse and human AHRs, resulting in differential transcriptional regulation of target genes (Flaveny *et al.*, 2008). As the factors comprising the AHR transcriptional complex become better understood, the study of ligand-dependent differential cofactor recruitment will likely provide mechanistic data to begin to understand human sensitivity or insensitivity to certain DLCs.

Although these mechanisms for differences in ligand-specific sensitivity between rat H4IIE cells and human keratinocytes are not clear, we do have the ability to measure human *in vitro* responses and rank the potency of DLCs in human cells, which we and others have shown are different from rodent responses *in vitro* and *in vivo*. Although this study did not exhaustively analyze all DLCs, we have been able to demonstrate that the differences in sensitivities between rodent and human cells are congener specific, indicating underlying complex molecular differences. Inclusion of human *in vitro* data in the evaluation of DLCs should allow scientists to more accurately determine the risk to human health from exposure to DLCs. This is especially important because TEFs are already being used in the exposure and human health assessment of TCDD and related compounds to determine risk of exposures to environmental mixtures of DLCs.

SUPPLEMENTARY DATA

Supplementary data are available online at http://toxsci.oxfordjournals.org/.

FUNDING

General Electric Company and the W. Harry Feinstone Center for Genomic Research.

ACKNOWLEDGMENTS

Real-time PCR was performed at the University of Tennessee Health Science Center Molecular Resource Center.

REFERENCES

Akaike, H. (1974). A new look at the statistical model identification. *IEEE Trans. Automat. Contr.* **19,** 716–723.

Bacon, D. W., and Watts, D. G. (1971). Estimating the transition between two intersecting straight lines. *Biometrika* **58,** 525–534.

Bailey, G. S., Orner, G. A., Pereira, C. B., and Swenberg, J. A. (2009a). Response to the Waddell et al. letter. *Chem. Res. Toxicol.* **22,** 1493–1494.

Bailey, G. S., Reddy, A. P., Pereira, C. B., Harttig, U., Baird, W., Spitsbergen, J. M., Hendricks, J. D., Orner, G. A., Williams, D. E., and Swenberg, J. A. (2009b). Nonlinear cancer response at ultralow dose: a 40800-animal ED(001) tumor and biomarker study. *Chem. Res. Toxicol.* **22,** 1264–1276.

Bars, R. G., and Elcombe, C. R. (1991). Dose-dependent acinar induction of cytochromes P450 in rat liver. Evidence for a differential mechanism of induction of P450IA1 by beta-naphthoflavone and dioxin. *Biochem. J.* **277**(Pt 2), 577–580.

Brenden, T. O., and Bence, J. R. (2008). Comment: use of piecewise regression models to estimate changing relationships in fisheries. *North Am. J. Fish. Manag.* **28,** 844–846.

Broccardo, C. J., Billings, R. E., Andersen, M. E., and Hanneman, W. H. (2005). Probing the control elements of the CYP1A1 switching module in H4IIE hepatoma cells. *Toxicol. Sci.* **88,** 82–94.

Broccardo, C. J., Billings, R. E., Chubb, L. S., Andersen, M. E., and Hanneman, W. H. (2004). Single cell analysis of switch-like induction of CYP1A1 in liver cell lines. *Toxicol. Sci.* **78,** 287–294.

Budinsky, R. A., Paustenbach, D., Fontaine, D., Landenberger, B., and Starr, T. B. (2006). Recommended relative potency factors for 2,3,4,7,8 pentachlorodibenzofuran: the impact of different dose metrics. *Toxicol. Sci.* **91,** 275–285.

Carlson, E. A., McCulloch, C., Koganti, A., Goodwin, S. B., Sutter, T. R., and Silkworth, J. B. (2009). Divergent transcriptomic responses to aryl hydrocarbon receptor agonists between rat and human primary hepatocytes. *Toxicol. Sci.* **112,** 257–272.

Ema, M., Ohe, N., Suzuki, M., Mimura, J., Sogawa, K., Ikawa, S., and Fujii-Kuriyama, Y. (1994). Dioxin binding activities of polymorphic forms of mouse and human arylhydrocarbon receptors. *J. Biol. Chem.* **269,** 27337–27343.

Environmental Protection Agency (EPA). (2009). *The U.S. Environmental Protection Agency's Strategic Plan for Evaluating the Toxicity of Chemicals* EPA 100/K-09/001, U.S. Environmental Protection Agency, Washington, DC.

Ertel, A., and Tozeren, A. (2008). Human and mouse switch-like genes share common transcriptional regulatory mechanisms for bimodality. *BMC Genomics* **9,** 628.

Fan, M. Q., Bell, A. R., Bell, D. R., Clode, S., Fernandes, A., Foster, P. M., Fry, J. R., Jiang, T., Loizou, G., MacNicoll, A., *et al.* (2009). Recombinant expression of aryl hydrocarbon receptor for quantitative ligand-binding analysis. *Anal. Biochem.* **384,** 279–287.

Feder, P. I. (1975a). On asymptotic distribution theory in segmented regression problems—identified case. *Ann. Stat.* **3,** 49–83.

Feder, P. I. (1975b). The log-likelihood ratio in segmented regression. *Ann. Stat.* **3,** 84–97.

Fernandez-Salguero, P. M., Hilbert, D. M., Rudikoff, S., Ward, J. M., and Gonzalez, F. J. (1996). Aryl-hydrocarbon receptor-deficient mice are resistant to 2,3,7,8-tetrachlorodibenzo-p-dioxin-induced toxicity. *Toxicol. Appl. Pharmacol.* **140,** 173–179.

Flaveny, C., Reen, R. K., Kusnadi, A., and Perdew, G. H. (2008). The mouse and human Ah receptor differ in recognition of LXXLL motifs. *Arch. Biochem. Biophys.* **471,** 215–223.

French, C. T., Hanneman, W. H., Chubb, L. S., Billings, R. E., and Andersen, M. E. (2004). Induction of CYP1A1 in primary rat hepatocytes by 3,3',4,4',5-pentachlorobiphenyl: evidence for a switch circuit element. *Toxicol. Sci.* **78,** 276–286.

Harper, P. A., Golas, C. L., and Okey, A. B. (1988). Characterization of the Ah receptor and aryl hydrocarbon hydroxylase induction by 2,3,7,8-tetrachlorodibenzo-p-dioxin and benz(a)anthracene in the human A431 squamous cell carcinoma line. *Cancer Res.* **48,** 2388–2395.

Haws, L. C., Su, S. H., Harris, M., Devito, M. J., Walker, N. J., Farland, W. H., Finley, B., and Birnbaum, L. S. (2006). Development of a refined database of mammalian relative potency estimates for dioxin-like compounds. *Toxicol. Sci.* **89,** 4–30.

Hedgeman, E., Chen, Q., Hong, B., Chang, C. W., Olson, K., Ladronka, K., Ward, B., Adriaens, P., Demond, A., Gillespie, B. W., *et al.* (2009). The University of Michigan dioxin exposure study: population survey results and serum concentrations for polychlorinated dioxins, furans, and biphenyls. *Environ. Health Perspect* **117,** 811–817.

Hestermann, E. V., Stegeman, J. J., and Hahn, M. E. (2000). Serum alters the uptake and relative potencies of halogenated aromatic hydrocarbons in cell culture bioassays. *Toxicol. Sci.* **53,** 316–325.

Hill, A. V. (1910). The possible effects of the aggregation of the molecules of haemoglobin on its dissociation curves. *J. Physiol.* **40,** iv–vii.

Hill, A. V. (1913). The combinations of haemoglobin with oxygen and with carbon monoxide. I. *Biochem. J.* **7,** 471–480.

Hinkley, D. V. (1969). Inference about the intersection in two-phase regression. *Biometrika* **56,** 495–504.

Hinkley, D. V. (1971). Inference in two-phase regression. *J. Am. Stat. Assoc.* **66,** 736–743.

Howard, G. J., Schlezinger, J. J., Hahn, M. E., and Webster, T. F. (2010). Generalized concentration addition predicts joint effects of aryl hydrocarbon receptor agonists with partial agonists and competitive antagonists. *Environ. Health Perspect.* **118,** 666–672.

Kenakin, T. (2007). Functional selectivity through protean and biased agonism: who steers the ship? *Mol. Pharmacol.* **72,** 1393–1401.

Knutson, J. C., and Poland, A. (1980). 2,3,7,8-Tetrachlorodibenzo-p-dioxin: failure to demonstrate toxicity in twenty-three cultured cell types. *Toxicol. Appl. Pharmacol.* **54,** 377–383.

Lerman, P. M. (1980). Fitting segmented regression models by grid search. *Appl. Stat.* **29,** 77–84.

Lindstrom, M. L., and Bates, D. M. (1990). Nonlinear mixed effects models for repeated measures data. *Biometrics* **46,** 673–687.

Lipp, H.-P., Schrenk, D., Wiesmüller, T., Hagenmaier, H., and Bock, K. W. (1992). Assessment of biological activities of mixtures of polychlorinated dibenzo-*p*-dioxins (PCDDs) and their constituents in human HepG2 cells. *Arch. Toxicol.* **66,** 220–223.

Lipshtat, A., Jayaraman, G., He, J. C., and Iyengar, R. (2010). Design of versatile biochemical switches that respond to amplitude, duration, and spatial cues. *Proc. Natl. Acad. Sci. U.S.A.* **107,** 1247–1252.

Lutz, W. K., and Lutz, R. W. (2009). Statistical model to estimate a threshold dose and its confidence limits for the analysis of sublinear dose-response relationships, exemplified for mutagenicity data. *Mutat. Res.* **678,** 118–122.

Michel, M. C., and Alewijnse, A. E. (2007). Ligand-directed signaling: 50 ways to find a lover. *Mol. Pharmacol.* **72,** 1097–1099.

Nagayama, J., Kiyohara, C., Masuda, Y., and Kuratsune, M. (1985). Inducing potency of aryl hydrocarbon hydroxylase activity in human lymphoblastoid cells and mice by polychlorinated dibenzofuran congeners. *Environ. Health Perspect.* **59,** 107–112.

National Research Council (NRC). (2007a). *Applications of Toxicogenomic Technologies to Predictive Toxicology and Risk Assessment.* National Research Council of the National Academies, The National Academies Press, Washington, DC.

National Research Council (NRC). (2007b). *Toxicity Testing in the Twenty-First Century: A Vision and a Strategy.* National Research Council of the National Academies, The National Academies Press, Washington, DC.

Peters, A. K., van Londen, K., Bergman, A., Bohonowych, J., Denison, M. S., Van den, B. M., and Sanderson, J. T. (2004). Effects of polybrominated diphenyl ethers on basal and TCDD-induced ethoxyresorufin activity and cytochrome P450-1A1 expression in MCF-7, HepG2, and H4IIE cells. *Toxicol. Sci.* **82,** 488–496.

Pfaffl, M. W. (2001). A new mathematical model for relative quantification in real-time RT-PCR. *Nucleic Acids Res.* **29,** e45.

Pinheiro, J. C., and Bates, D. M. (2004). In *Mixed-Effects Models in S and S-Plus.* Springer Science and Business Media, New York, NY.

Poland, A., and Knutson, J. C. (1982). 2,3,7,8-Tetrachlorodibenzo-p-dioxin and related halogenated aromatic hydrocarbons: examination of the mechanism of toxicity. *Annu. Rev. Pharmacol. Toxicol.* **22,** 517–554.

R Development Core Team. (2006). *R: A Language and Environment for Statistical Computing,* Version 2.10.1. R Foundation for Statistical Computing, Vienna, Austria. Available at: http://www.R-project.org.

Ramadoss, P., and Perdew, G. H. (2004). Use of 2-azido-3-[125I]iodo-7, 8-dibromodibenzo-p-dioxin as a probe to determine the relative ligand affinity of human versus mouse aryl hydrocarbon receptor in cultured cells. *Mol. Pharmacol.* **66,** 129–136.

Seber, G. A. F., and Wild, C. J. (2003). In *Nonlinear Regression.* John Wiley & Sons, Inc., Hoboken, NJ.

Silkworth, J. B., Koganti, A., Illouz, K., Possolo, A., Zhao, M., and Hamilton, S. B. (2005). Comparison of TCDD and PCB CYP1A induction sensitivities in fresh hepatocytes from human donors, Sprague-Dawley rats, and rhesus monkeys and HepG2 cells. *Toxicol. Sci.* **87,** 508–519.

Slob, W. (2007). What is a practical threshold? *Toxicol. Pathol.* **35,** 848–849.

Sobels, F. H. (1980). Evaluating the mutagenic potential of chemicals. The minimal battery and extrapolation problems. *Arch. Toxicol.* **46,** 21–30.

Sutter, C. H., Rahman, M., and Sutter, T. R. (2006). Uncertainties related to the assignment of a toxic equivalency factor for 1,2,3,4,6,7,8,9-octachlorodibenzo-p-dioxin. *Regul. Toxicol. Pharmacol.* **44,** 219–225.

Sutter, C. H., Yin, H., Li, Y., Mammen, J. S., Bodreddigari, S., Stevens, G., Cole, J. A., and Sutter, T. R. (2009). EGF receptor signaling blocks aryl hydrocarbon receptor-mediated transcription and cell differentiation in human epidermal keratinocytes. *Proc. Natl. Acad. Sci. U.S.A.* **106,** 4266–4271.

Toms, J. D., and Lesperance, M. L. (2003). Piecewise regression: a tool for identifying ecological thresholds. *Ecology* **84,** 2034–2041.

Toyoshiba, H., Walker, N. J., Bailer, A. J., and Portier, C. J. (2004). Evaluation of toxic equivalency factors for induction of cytochromes P450 CYP1A1 and CYP1A2 enzyme activity by dioxin-like compounds. *Toxicol. Appl. Pharmacol.* **194,** 156–168.

Tritscher, A. M., Goldstein, J. A., Portier, C. J., McCoy, Z., Clark, G. C., and Lucier, G. W. (1992). Dose-response relationships for chronic exposure to 2,3,7,8-tetrachlorodibenzo-p-dioxin in a rat tumor promotion model: quantification and immunolocalization of CYP1A1 and CYP1A2 in the liver. *Cancer Res.* **52,** 3436–3442.

Uno, S., Dalton, T. P., Sinclair, P. R., Gorman, N., Wang, B., Smith, A. G., Miller, M. L., Shertzer, H. G., and Nebert, D. W. (2004). Cyp1a1(-/-) male mice: protection against high-dose TCDD-induced lethality and wasting syndrome, and resistance to intrahepatocyte lipid accumulation and uroporphyria. *Toxicol. Appl. Pharmacol.* **196,** 410–421.

Urban, J. D., Clarke, W. P., von Zastrow, M., Nichols, D. E., Kobilka, B., Weinstein, H., Javitch, J. A., Roth, B. L., Christopoulos, A., Sexton, P. M., *et al.* (2007). Functional selectivity and classical concepts of quantitative pharmacology. *J. Pharmacol. Exp. Ther.* **320,** 1–13.

Vamvakas, A., Keller, J., and Dufresne, M. (1996). In vitro induction of Cyp1a1-associated activities in human and rodent cell lines by commercial and tissue-extracted halogenated aromatic hydrocarbons. *Environ. Toxicol. Chem.* **15,** 814–823.

Van den Berg, M., Birnbaum, L. S., Denison, M., De Vito, M., Farland, W., Feeley, M., Fiedler, H., Hakansson, H., Hanberg, A., Haws, L., *et al.* (2006). The 2005 World Health Organization re-evaluation of human and mammalian toxic equivalency factors for dioxins and dioxin-like compounds. *Toxicol. Sci.* **93,** 223–241.

Westerink, W. M., Stevenson, J. C., and Schoonen, W. G. (2008). Pharmacologic profiling of human and rat cytochrome P450 1A1 and 1A2 induction and competition. *Arch. Toxicol.* **82,** 909–921.

Williams, D. E., Orner, G., Willard, K. D., Tilton, S., Hendricks, J. D., Pereira, C., Benninghoff, A. D., and Bailey, G. S. (2009). Rainbow trout (Oncorhynchus mykiss) and ultra-low dose cancer studies. *Comp. Biochem. Physiol. C Toxicol. Pharmacol.* **149,** 175–181.

Wilson, C. L. (2004). Molecular switch circuits in toxicology: a dimmer switch for dioxin. *Toxicol. Sci.* **78,** 178–180.

Yanagimoto, T., and Yamamoto, E. (1979). Estimation of safe doses: critical review of the hockey stick regression method. *Environ. Health Perspect.* **32,** 193–199.

Zeiger, M., Haag, R., Hockel, J., Schrenk, D., and Schmitz, H. J. (2001). Inducing effects of dioxin-like polychlorinated biphenyls on CYP1A in the human hepatoblastoma cell line HepG2, the rat hepatoma cell line H4IIE, and rat primary hepatocytes: comparison of relative potencies. *Toxicol. Sci.* **63,** 65–73.

Zhang, S., Rowlands, C., and Safe, S. (2008). Ligand-dependent interactions of the Ah receptor with coactivators in a mammalian two-hybrid assay. *Toxicol. Appl. Pharmacol.* **227,** 196–206.